2 Ultrasound-Guided Regional Anaesthesia: Visualising the Nerve and Needle

James Bowness and Alasdair Taylor

Abstract

Regional anaesthesia involves targeting specific peripheral nerves with local anaesthetic. It facilitates the delivery of anaesthesia and analgesia to an increasingly complex, elderly and co-morbid patient population. Regional anaesthesia practice has been transformed by the use of ultrasound, which confers advantages such as accuracy of needle placement, visualisation of local anaesthetic spread, avoidance of intraneural injection and the ability to accommodate for anatomical variation.

An US beam is generated by the application of electrical current to an array of piezoelectric crystals, causing vibration and consequential production of high-frequency sound waves. The sound energy is reflected at tissue interfaces, detected by the piezoelectric crystals in the ultrasound probe, and most frequently displayed as a 2D image.

Optimising image acquisition involves selection of the appropriate US frequency: this represents a trade-off between image resolution (better with high frequency) and tissue penetration/beam attenuation (better with low frequency). Altering alignment, rotation and tilt of the probe is often required to optimise the view as nerves are best visualised when the ultrasound beam is directly perpendicular to their fibres. Adjusting the focus, depth, and gain (brightness) of the image display can also help in this matter.

Three key challenges exist in regional anaesthesia; image optimisation, image interpretation (nerve visualisation) and needle visualisation. There are characteristic sonographic appearances of the nerve structures for peripheral nerve blocks, as discussed in this chapter, and the above techniques can be used to enhance their appearance. Much research has been done, and is ongoing, with the aim of improving needle visualisation; this is also reviewed. Image interpretation requires the application of anatomical knowledge and understanding of the typical sonographic appearance of different tissues (as well as the needle). Years of practice are required to attain expertise, although it is hoped that continuing

Illustrators

Ross Jones University of Edinburgh, Edinburgh, Scotland, UK

Filip Zmuda University of Dundee, Dundee, Scotland, UK

J. Bowness (✉)
University of Dundee, Dundee, Scotland, UK

NHS Tayside, Dundee, Scotland, UK

Department of Anaesthesia, Level 6, Ninewells Hospital, Dundee, Scotland, UK
e-mail: james.bowness@nhs.net

A. Taylor
NHS Tayside, Dundee, Scotland, UK
e-mail: alasdairtaylor1@nhs.net

P. M. Rea (ed.), *Biomedical Visualisation*, Advances in Experimental Medicine and Biology 1235,
https://doi.org/10.1007/978-3-030-37639-0_2

advances in nerve and needle visualisation, as described in this chapter, will expedite that process.

Keywords
Ultrasound · Regional anaesthesia · Anatomy · Visualisation · Anatomical variation · Image analysis · Nerve · Needle

Abbreviations

CNB	central neuroaxial blockade
GA	general anaesthesia/anaesthetic
LA	local anaesthesia/anaesthetic
RA	regional anaesthesia/anaesthetic
UGRA	ultrasound-guided regional anaesthesia
US	ultrasound

2.1 Introduction

The triad of anaesthesia includes hypnosis (reduction of awareness), analgesia, and paralysis/lack of movement. This aims to achieve a state that is acceptable to patients undergoing a controlled trauma (i.e. surgical procedure), and provide optimal conditions for the operating surgeon (e.g. lack of movement, bleeding etc).

There are several methods to achieve this. **General anaesthesia** (GA) uses intravenous and/or inhalational pharmacological agents to induce a controlled state of unconsciousness. These drugs, with or without the addition of agents to produce muscle paralysis and analgesia, achieve the conditions described above. For **central neuraxial blockade** (CNB), local anaesthetic (LA) is deposited around nerves of the central nervous system to block sensory stimuli conveyed to the brain and motor stimuli conveyed to the muscles. It may be used to achieve anaesthesia suitable for surgical procedures (e.g. caesarean section under spinal anaesthesia) or analgesia (e.g. epidural in labour). Examples of CNB include spinal, epidural and caudal anaesthesia. During **regional anaesthesia** (RA), anaesthetists target specific peripheral nerves with LA injections in order to block the sensorimotor stimuli conveyed. This allows selective anaesthesia of body regions during surgery and for analgesia in the post-operative period. This can be advantageous for patients in whom GA presents a high risk of morbidity or mortality, and for particularly painful procedures or patients with chronic pain conditions. **Local anaesthesia** involves infiltration of LA within tissues targeted during a surgical procedure (e.g. LA infiltration into cutaneous tissue to remove a skin lesion). These techniques may be used in isolation or, more commonly, in combination – often with the addition of other systemic agents such as analgesics and anti-emetics.

Ultrasound (US) guidance has transformed RA in the twenty-first century, allowing direct and real-time visualisation of the structures involved. It has enabled anaesthetists to employ RA techniques, more frequently and in more diverse scenarios, as a tool to combat the challenges presented by an increasingly elderly, co-morbid and obese patient population. This chapter will review the principles of US used in **ultrasound-guided regional anaesthesia** (UGRA) and the descriptions of US images for specific **peripheral nerve blocks** (PNBs) of the upper and lower limb. Particular focus will be on the appearance of nerve structures and methods to optimise visualisation of the nerve which demonstrate the principles first discussed. The difficulties in needle identification will also be reviewed, as well as strategies and new technologies that are in development to help identify needles on ultrasound.

2.2 Regional Anaesthesia

Historically, such techniques relied on knowledge of anatomical landmarks to guide needle placement and deposition of LA. However, this approach was prone to inadequate efficacy and associated with greater potential risks, partly because peripheral nerves are naturally subject to structural variation meaning that accurate perineurial deposition of LA was not always achieved. Equally, variation in the vascular anatomy can predispose to inadvertent blood vessel trauma, with potential bleeding and intravascular injection of LA, risking LA systemic toxicity.

Initial attempts to improve accuracy of perineurial LA deposition included the use of nerve stimulators to elicit a motor (muscle twitch) or sensory (paraesthesia) response of the target nerve. This improved efficacy but did not mitigate for anatomical variance or inadvertent damage to surrounding structures. More recently US has emerged as the predominant strategy to guide RA techniques. Potential advantages of visualising the area of interest in real time include accuracy of needle placement, visualisation of LA spread, avoidance of intraneural injection and reduced complications/trauma to surrounding structures by observing the needle along its entire course (Coventry and Raju 2016; Munimara and McLeod 2015; Henderson and Dolan 2018). Also, and fundamentally, UGRA is intended to allow compensation for anatomical variation by directly visualising the anatomy and so allow appropriate direction of the needle/injection toward target nerves (Coventry and Raju 2016; Henderson and Dolan 2018; Griffin and Nicholls 2010). Such benefits have been demonstrated to improve efficacy (Munimara and McLeod 2015), and US is known to be safe, non-ionising and non-painful. However, it is also known to be subjective and published data demonstrates that nerve identification on ultrasound is imperfect even by experienced anaesthetists with advanced training in regional anaesthesia (Bowness et al. 2019). Identification of needle position is another challenge in UGRA, particularly when the needle is inserted at a steep angle to the US probe as is necessary in some deeper blocks (e.g. infraclavicular brachial plexus block).

2.3 Principles of Ultrasound Used in Regional Anaesthesia

The principles of US have been discussed elsewhere in this series, hence only a brief review will be included here. For more details see (Varsou 2019).

Ultrasound uses electrical current to cause vibration in piezoelectric crystals on the end of a transducer probe. This vibration generates a beam of high-frequency sound waves (2–18 MHz in UGRA), which are inaudible to the human ear. As they travel through the body, they are reflected at tissue interfaces as different tissue types/densities transmit or reflect the sound waves to differing extents. Reflected sound waves are received at the probe and generate a separate vibration in the piezoelectric crystals of the ultrasound probe (proportional to the strength of the sound waves received). These, in turn, generate an electrical current in the transducer, the amplitude of which is proportional to the vibration of the piezoeletric crystals (A-mode). When a series of transducers are placed in alignment on a probe, this can be displayed on a screen as a two-dimensional image, with the strength of signal received (amplitude, A-mode) expressed as brightness on a screen (B-mode). Other modes are used in clinical practice but B-mode is the most common, particularly in UGRA. As sound waves travel at almost constant speed through body tissues (1540 m/sec +/−5%) (Townsley et al. 2014; Smith et al. 2017), the depth at which sound waves are reflected is calculated by the time taken for a signal to return to the transducer.

The frequency of US represents a trade-off between resolution (i.e. the ability to distinguish between two points at a particular depth) and attenuation (i.e. the reduction in amplitude of the US beam as it passes through the body tissue). Higher frequency, shorter wavelength, sound waves provide better image resolution, but undergo greater attenuation as they pass through the tissues. In practical terms, this means that high US frequencies are most appropriate for superficial structures, with a greater ability to visualise small structure (e.g. small nerves, fine needles). Conversely, lower frequencies are better for imaging deeper structures but have a lower resolution (and consequently a lesser ability to visualise small anatomical detail and fine needles).

2.4 Image Optimistion

One can adjust the **pressure** with which the transducer probe is applied to the skin, to achieve the optimal tissue visualisation whilst minimising tissue distortion. Intermittent pressure can be helpful to confirm identification of tissues visualised, as blood vessels and nerves can be similar in appearance. Veins are compressible due to their low pressure, therefore gentle pressure applied through the probe will obliterate a venous lumen, whereas arteries and nerves cannot be easily compressed. Pressure can augment the characteristic expansile/pulsatile appearance of arteries, which is not a feature of neural tissue.

Moving (sliding) the probe over the skin enables one to trace structures proximally or distally, and therefore aid in confirming their identity, and determine the orientation of nerve fibres (or muscle fibres/the lumen of blood vessels). This allows the operator to **align** the probe appropriately and identify the optimal site for needle entry during nerve block. It should be emphasised that US identification of structures is a **dynamic** process and it is often difficult to confidently identify structures on a single image. Tracing the hyper/hypoechoic focus along its course, and comparing it to anatomical relations, is an important component of confirming structure identification. Note that US machines display magnified images and very small movements are amplified on screen. Thus, very small probe movements may translate to large changes in the image displayed, including losing view of the target nerve (or needle) altogether. Mitigating unwanted movements during block performance comes with increasing operator experience.

Rotation (twisting) the US probe allows operators to confirm the orientation of fibres in a nerve or muscle, or the lumen of a blood vessels. This enables visualisation of the nerve in short axis (cross section) or long axis (longitudinal) view (Fig. 2.1). In UGRA, target nerves are most commonly visualised in short axis/cross section: this allows better identification of the structure during needle advancement as well as perineurial spread of local anaesthetic. Nerve trauma and intra-neural injection is also more readily identified in short axis.

Tilting the angle of **insonation** (angle of incidence) of the US probe to the skin

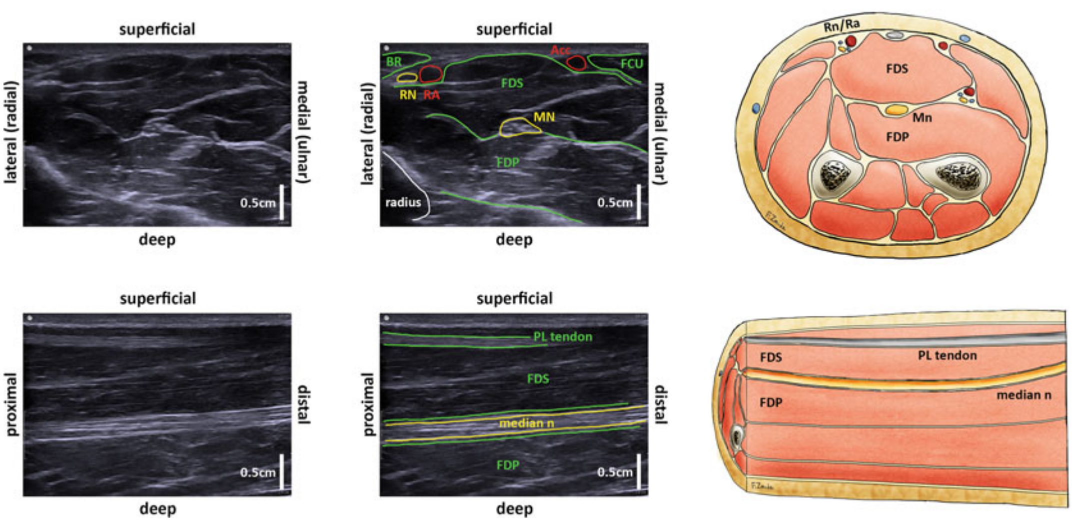

Fig. 2.1 Median nerve
Top: median nerve in short axis (L to R: unlabelled US; labelled US; illustration)
Bottom: median nerve in long axis (L to R: unlabelled US; labelled US; illustration)
(*Acc* accessory artery; *BR* brachioradialis, *FCU* flexor carpi ulnaris; *FDP* flexor digitorum profundus; *FDS* flexor digitorum superficialis; *Mn/MN/median* n median nerve; *PL* palmaris longus; *Ra/RA* radial artery; *Rn/RN* radial nerve)

alters the visualisation of target structures seen in short axis. Nerves display anisotropy (their visualisation by ultrasound is dependent upon the angle of inclination of the ultrasound beam); they are best visualised with the probe at 90° to them to maximise the amount of signal returned. They are poorly visualised with an angle of insonation of <60° (Townsley et al. 2014). Carefully rocking the US probe (adjusting the angle of insonation of the long axis) can be used to improve visualisation of structures seen in long axis.

Other features of US, which can be used to confirm identification of structures visualised include the **Doppler effect** (discussed in more detail elsewhere in this series – Varsou 2019). Objects travelling toward the transducer reflect US waves back toward it at a higher frequency/shorter wavelength than when they struck the object. The opposite is true of objects travelling away from the transducer (a common example is an ambulance passing an observer: the tone of the siren changes as the vehicle approaches and then drives past). The most common example of this in the human body is blood flow in blood vessels: the change in frequency can be detected and colour applied to the altered frequency. Reduced frequency (movement away from the scanner) is shown in blue, with increased frequency (movement towards the transducer) in red. This leads to the acronym BART (blue away, red towards) and can be applied to real-time images to identify blood flow in vessels, which helps distinguish them from nerves (which show no Doppler shift). It is important to note that a Doppler shift will not occur when the angle of insonation is exactly 90°, as movement of structures in a purely perpendicular plane will not change the frequency of soundwaves reflected.

Setting the **focus** of the US beam alters the pattern of US waves emitted by the transducer, so the sound waves are at the greatest intensity a set depth, to optimise resolution at the **depth** of the target tissue. The **gain** (brightness) of the display can also be used to optimise the display of the image acquired.

2.5 General Appearance of Peripheral Nerves on Ultrasound

Neural tissue is hypoechoic and connective tissue hyperechoic. Therefore, nerves contain both of these elements in their appearance. They generally contain a higher proportion of neural tissue at locations more proximate to the central nervous system and so appear as round hypoechoic structures (in short axis). More distally, they have a heterogeneous 'speckled' or 'honeycomb' appearance; a hyperechoic outline (epineurium) with matrix of perineurium and connective tissue, and hypoechoic speckles of neural tissue within (Fig. 2.1). More peripheral nerves are also shaped by the surrounding structures, and so less rounded. In long axis, these nerves display a striated appearance.

Muscle tissue also contains hypoechoic fascicles with hyperechoic epimysium and perimysium. It is generally relatively easy to distinguish between this and the nerve tissue, however, as muscles generally have a much greater cross sectional area and their fascicles are larger. Muscle tendons can appear similar to peripheral nerves, but become more hyperchoic as they approach their insertion (and blend with the body of the muscle, with a flatter appearance, when scanning away from it). Blood vessels are anechoic, as fluid is a very weak reflector of US, appearing black on a B-mode image. As discussed above, veins are easily compressible whilst arteries are pulsatile (they are actually expansile, but this can sometimes be harder to see than the pulsation). Arteries are also round, with thicker walls, whereas veins have a more irregular outline which is shaped somewhat by the surrounding structures due to the thin venous wall and low pressure.

2.6 Nerve Appearance: Upper Limb Nerve Blocks

2.6.1 Interscalene Block

This block is commonly performed for surgery on the shoulder as it aims to deposit LA around the C5/6/7 nerve roots in the plane between scalenus anterior and medius (Raju and Bowness 2019). It uses a linear transducer, placed transversely on the anterolateral skin of the neck, approximately at the level of C6 (the cricoid cartilage). This is an example of imaging proximate peripheral nerves, which contain only a small amount of connective tissue and hence appear as rounded hypoechoic structures (Fig. 2.2). The phrenic nerve can be seen anteromedial to the cervical nerve roots, as a small hypoechoic region on the superficial surface of scalenus anterior. The vertebral artery and vein lie deep to scalenus anterior and the nerve roots, and can be identified with colour flow Doppler and by the arterial pulsation.

2.6.2 Supraclavicular Block

This block allows injection of LA around the distal trunks/proximal divisions of the brachial plexus. By placing a linear transducer in a coronal oblique orientation in the supraclavicular fossa, one can view the brachial plexus nerve trunks/divisions lying superior and posterolateral to the subclavian artery (Raju and Bowness 2019). The nerves again appear as hypoechoic structures, often in a common fascial sheath (with an appearance resembling a 'bunch of grapes'), lying above the dome of the pleural and over the first rib (Fig. 2.3). Anterior to them is the insertion of

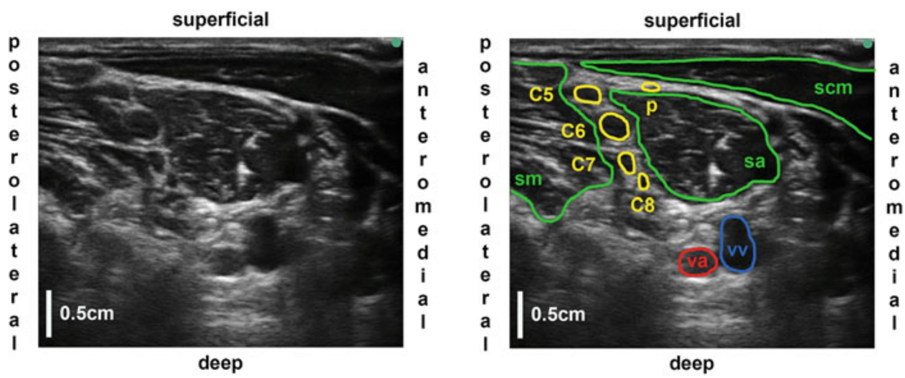

Fig. 2.2 US view during an interscalene block. (Reproduced with permission from Bowness & Taylor, Anatomy for the FRCA, 2019 ©)
(*p* phrenic nerve; *sa* scalenus anterior; *scm* sternocleidomastoid; *sm* scalenus medius; *va* vertebral artery; *vv* vertebral vein)

Note: Directing the probe slightly inferiorly may enhance visualisation of the nerve roots, as they themselves travel somewhat inferiorly as they leave the intervertebral foramina. Also, the nerves may not lie in the typical distribution described above. It is not infrequent to find them lying in another pattern, sometimes travelling through one of the scalene muscles

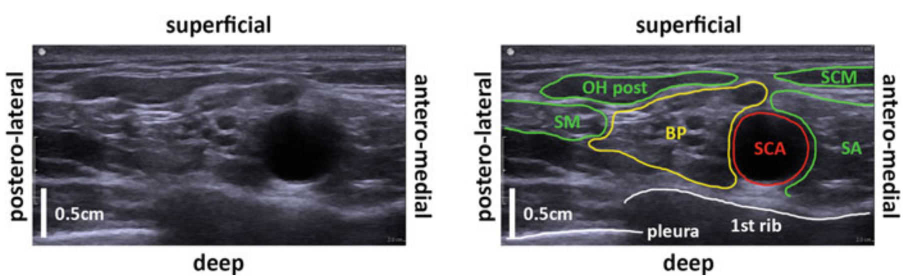

Fig. 2.3 US view during a supraclavicular block
(*BP* brachial plexus, *OH* post posterior belly of omohyoid, *SA* scalenus anterior, *SCA* subclavian artery, *SCM* sternocleidomastoid, *SM* scalenus medius)
Note: It is important to avoid damage to underlying pleura when inserting the block needle. Bone has a high acoustic impedance and so reflects sound waves effectively. It therefore appears hyperechoic with an acoustic shadow deep to it. The pleura also appears bright, but without the same degree of hypoechoic signal deep to it – the two layers of pleural can also be seen to move during respiration. The dorsal scapular and transverse cervical arteries are in the vicinity of the needle route - it may be possible to recognise these by identifying the characteristic arterial features on ultrasound, including colour Doppler

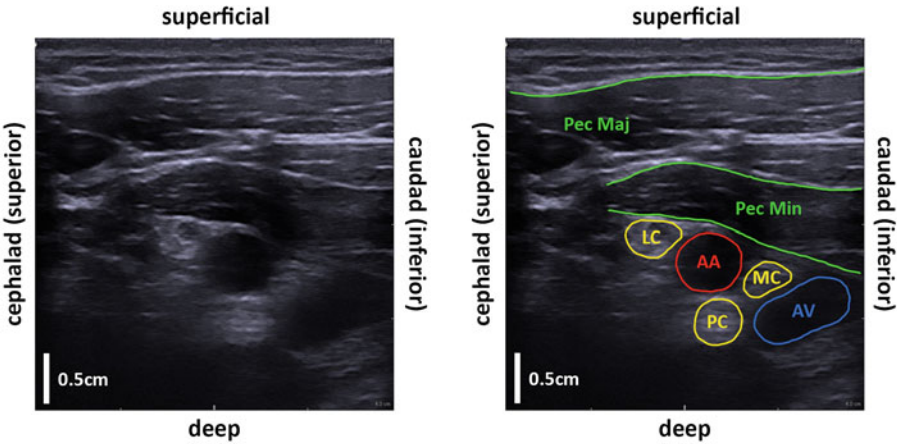

Fig. 2.4 US view during an infraclavicular block (*AA* axillary artery; *AV* axillary vein; *LC* lateral cord; *MC* medial cord; *PC* posterior cord; *Pec maj* pectoralis major muscle; *Pec Min* pectorals minor muscle)
Note: The cords initially lie lateral to the axillary artery, then in the characteristic distribution surrounding the artery as they move inferolaterally. The posterior cord can be difficult to visualise, masked by an area of image artefact deep to the artery (post-cystic enhancement). If this is the case, visualising a perivascular spread of LA deposition can be used to achieve the required block. The angle of needle insertion required can make needle visualisation difficult; as is it inserted caudad to the clavicle and travels steeply, deep to the probe. Techniques to overcome this include use of an echogenic needle (see below), curvilinear probe and rocking the probe (applying greater pressure at the inferior end of the probe to align it to the axis of the needle)

scalenus anterior (onto the scalene tubercle of the first rib) and then the subclavian vein. Scalenus medius can be seen posteriorly.

2.6.3 Infraclavicular Block

To best view the cords of the brachial plexus around the artery, align the probe with the long axis in the sagittal plane and place it in the infraclavicular fossa (below the coracoid process). The pectoralis muscles are the most superficial major structures encountered, with their muscle fibres travelling in different planes: pectoralis major visualised in short axis and pectoralis minor in long axis. Deep to this lie the cords and artery, and at this point the nerves have begun to develop the speckled appearance of hyperechoic connective tissue containing hypoechoic neural tissue (Fig. 2.4). The lateral cord lies cephalad to the artery (lateral, anterior and superior), in the 9–11 o'clock position on the US view described. The posterior cord lies deep (inferomedial, 6 o'clock) and the medial cord lies inferomedial (2–3 o'clock) (Raju and Bowness 2019).

2.6.4 Axillary Brachial Plexus Block

This block is performed at the level of the proximal, medial arm (begin by visualising the axillary artery as proximally as possible). The nerves targeted are the musculocutaneous, median, ulnar and radial nerves.[1] Interestingly, they often appear not as one structure itself, but a number of neural bundles – often larger than one would expect. The musculocutaneous nerve no longer lies in a perivascular location and is found in a fascial plane between the short head of biceps and coracobrachialis (Fig. 2.5). This is an example of the benefit of dynamic scanning: following the nerve proximally and distally can allow it to be viewed moving laterally as it leaves the neurovascular bundle and takes up its position between the two muscle bellies more distally in the arm. The median nerve is usually seen on the anterolateral side of the artery, in the 9–12 o'clock

[1] The medial cutaneous nerves of the arm and forearm, as well as the intercostobrachial nerves, are not usually seen but targeted by a subcutaneous infiltration of LA in the proximal, medial arm.

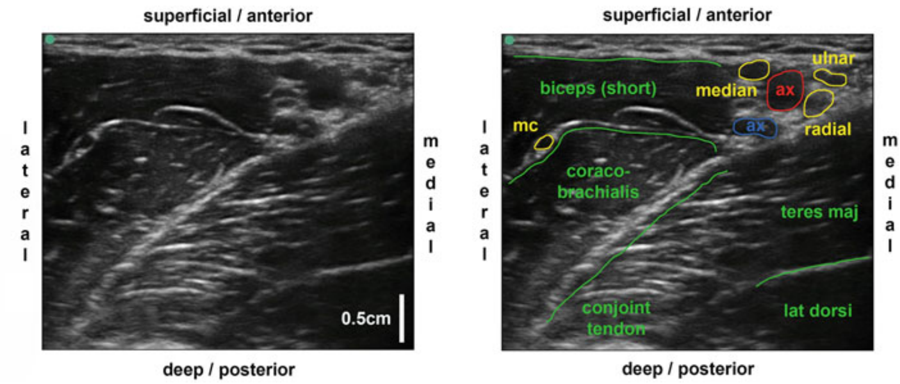

Fig. 2.5 US view during an axillary level brachial plexus block. (Reproduced with permission from Bowness & Taylor, Anatomy for the FRCA, 2019 ©)
(*mc* musculocutaneous nerve, *ax* (blue) axillary vein, *ax* (red) axillary artery)
Note: The radial nerve is most difficult to visualise because it does not lie perpendicular to the probe position: performing the block proximally in the arm and adjusting the rotation/tilt of the probe may aid in viewing it. Post-cystic enhancement, deep to the artery, may further compound difficulties with image interpretation. To help with identification, all the nerves can be traced from more distal positions to their final locations relative to the artery (Raju and Bowness 2019). The number and distribution of nerves and blood vessels in the region is variable (Townsley et al. 2014) and they can have a similar appearance. Colour Doppler can be used to discriminate between vascular and neural structures, and compression of veins allows better visualisation of deep structures (eliminating the post-cystic enhancement)

position (on the biceps side). The ulnar nerve is more varied: it is usually found on the medial side, but may lie anterolateral (1–3 o'clock) or slightly posterior/deeper (on the triceps side of the artery). The radial nerve is generally found deep to the ulnar nerve, sometimes on the anterior surface of the conjoint tendon of teres major/latissimus dorsi (Raju and Bowness 2019).

2.6.5 Forearm Blocks

The radial, median and ulnar nerves can be identified and blocked at or below the elbow. The radial nerve is best found on the lateral side of the limb, just above the elbow crease (on the lateral border of brachialis muscle, between it and coracobrachialis). The median nerve can be found in the mid-forearm, on the deep surface of flexor digitorum superficialis (superficial to flexor digitorum profundus). The ulnar nerve lies deep to flexor carpi ulnaris and approaches the medial side of the ulnar artery: this can be a useful landmark to find the nerve, which can then be traced proximally until the artery and nerve diverge. At these point, all the nerves appear heterogenous in short axis, with hyperechoic borders and elements of hypoechoic neural tissue within (Fig. 2.1).

2.7 Nerve Appearance: Lower Limb Nerve Blocks

2.7.1 Femoral Nerve Block

The femoral nerve passes into the thigh under the mid-point of the inguinal ligament (midway between the pubic tubercle and anterior superior iliac spine), lateral to the femoral artery (which travels under the ligament at the mid-inguinal point; midway between the pubic symphysis and the anterior superior iliac spine) (Bowness and Taylor 2019). As a branch of the lumbosacral plexus, it receives contributions from the nerve roots of L2/3/4, and fours within psoas major muscle. It therefore passes into the lower limb deep to the fascia iliaca (the fascia over iliacus muscle), which is continuous with psoas fascia (the fascia over psoas major) as these two muscles have a common tendinous insertion on the lesser trochanter of the femur.

Using a linear transducer placed transversely across the proximal anterior thigh, the femoral

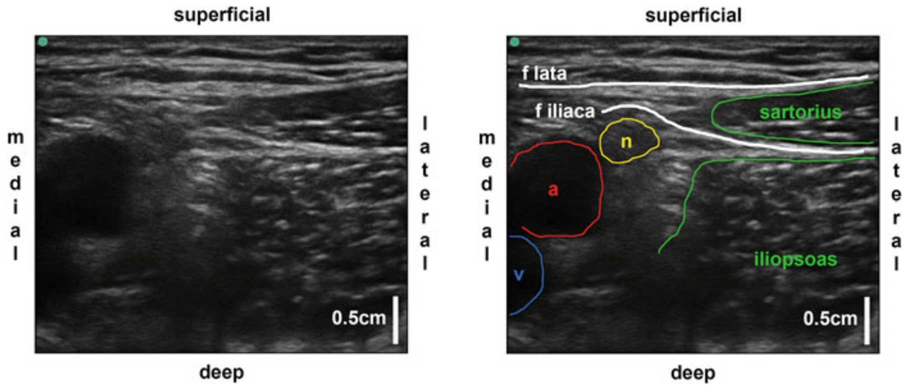

Fig. 2.6 US view during a femoral nerve block. (Reproduced with permission from Bowness & Taylor, Anatomy for the FRCA, 2019 ©)
(*a* femoral artery; *n* femoral nerve; *v* femoral vein)
Note: As the femoral nerve does not travel exactly parallel to the femoral vessels, it may be difficult to obtain a single image that optimises the view for all three. The nerve is often best visualised in the same plane at the fascia iliaca, and tilting the probe slowly back and forth may aid identification. The nerve boundaries often become clearer after beginning to inject LA at which point it can separate from the fascia (hydrodissection)

vessels are a useful landmark to visualise. The artery can be seen pulsating (and identified with colour Doppler) and, on its medial side, lies the femoral vein (it may lie slightly deep to the artery and is compressible). Lateral to these vessels it is possible to identify two fascial layers: the fascia lata (the deep investing fascia of the thigh) and fascia iliaca (the fascia overlying iliacus/iliopsoas muscle). The fascia lata is the more superficial layer and can be followed medially, passing anterior to the femoral artery. The fascia iliaca passes deep to the artery (Fig. 2.6). Deep to both, and lateral to the artery, lies the femoral nerve (on the superficial surface of iliacus/iliopsoas), which is said to travel in a tunnel on the deep surface of fascia iliaca. It often appears hyperechoic, and oval or triangular in cross-section (Grant 2019).

2.7.2 Popliteal Sciatic Nerve Block

This block targets the sciatic nerve, at the point where it divides into the tibial and common peroneal nerves (Grant 2019). This division is traditionally said to occur at the apex above the popliteal fossa, where the muscle bellies of semimembranosus (medially) and biceps femoris (laterally) come together. However, the nerve can separate into these two discrete structures at any point in the posterior thigh, although usually travels in a common epineurial sheath to a point within about a hand's breath above the popliteal skin crease.

By placing a linear transducer transversely on the posterior skin of the thigh, just above the popliteal skin crease, one can view the neurovascular bundle. The popliteal artery is the deepest structure in the popliteal fossa, with the compressible popliteal vein superficial to it. The tibial nerve has the classical 'honeycomb' spiculated appearance, with a bright echogenic architecture containing hypoechoic nerve fascicles (Fig. 2.7). Again, the nerve displays anisotropy, so altering the tilt of the probe (without moving it proximally/distally along the limb) will enhance/degrade the visualisation of the nerve. After optimising the view of the tibial nerve, it can be traced proximally to the point at which the common peroneal nerve joins it from the lateral side (from adjacent to/under the biceps femoris muscle).

2.7.3 Ankle Block

Five nerves are targeted in this block: the tibial, deep peroneal (fibular), superficial peroneal (fibular), saphenous and sural nerves. They display the typical 'honeycomb' appearance of distal

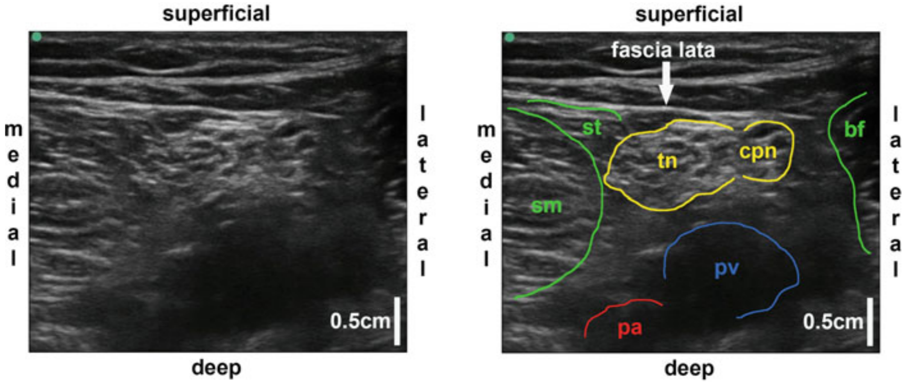

Fig. 2.7 US view during a popliteal level sciatic nerve block. (Reproduced with permission from Bowness & Taylor, Anatomy for the FRCA, 2019 ©)
(*sm* semimembranosus muscle; *st* semitendinosus muscle; *tn* tibial nerve; *cpn* common peroneal nerve; *pa* popliteal artery; *pv* popliteal vein; *bf* biceps femoris)
Note: This block is another example where hydrodissection enhances visualisation of the nerves following injection of LA under the surrounding fascial sheath - giving a classic dark 'halo' of LA with the bright nerve structures in the middle

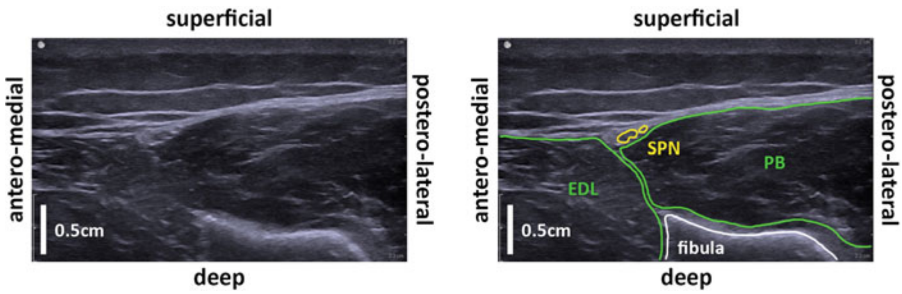

Fig. 2.8 US view of the superficial peroneal nerve on US
(*EDL* extensor digitorum longus; *PB* peroneus brevis; *SPN* superficial peroneal nerve)

peripheral nerves on ultrasound, with echogenic connective tissue (accounting for a steadily larger portion of the nerve) and hypoechoic nerve fascicles (Fig. 2.8).

2.8 Strategies to Aid Nerve Identification on Ultrasound

As is seen from the figures above, US image interpretation during UGRA takes training and experience. However, training in UGRA is often *ad hoc*, with experience gained incrementally over many years (often with different trainers and without structured, specific goals). Therefore, the pedagogical practice may contribute to this problem and education/training can play a significant role to overcome the difficulties in needle (and nerve) visualisation. A recent trend of mastery learning, with deliberate and iterative practice, is one example of such training.

In addition, the US image obtained in the same patient/PNB will vary considerably with small changes in position or angulation of the probe, and interpretation still involves a degree of subjectivity. Publications demonstrate imperfect human analysis of medical images, even amongst experts attempting to identify very obvious anomalies (Drew et al. 2013). This is particularly pertinent to UGRA when anatomical variation presents anomalous topography of peripheral nerves – expert identification of peripheral nerves is known to be imperfect and may contribute to the failure rate of RA techniques (Bowness et al.

2019). Therefore, the field is in need of strategies to improve nerve identification during UGRA.

One method to compliment nerve identification, and avoid nerve trauma/intraneural injection, is the practice of placing nerve blocks in awake patients where possible. Although this does not improve visualisation of the nerve (or needle), early detection of complications (e.g. pain or paraesthesia on injection/nerve contact by the needle) can aid in minimising the risk of serious nerve injury. However, awake patients are more prone to moving and it therefore is important to maintain a dialogue with the patient throughout the procedure to improve patient compliance and reduce unwanted movement.

Unfortunately, despite the potential for inaccuracy in nerve identification on US to impair the efficacy of UGRA techniques, there is a relative paucity of research on new technologies to aid in this task. Although there are individual benefits of nerve stimulation and US-guidance, combining these existing technologies when performing PNB does not appear to further reduce the rate of nerve injury (Munimara and McLeod 2015). Recent work on the use of micro-ultrasound as a tool to image peripheral nerves during regional anaesthesia shows promise (Chandra et al. 2017). However, the definition of micro-ultrasound in this study was anatomical resolution better than 100 μm, and nerve fascicles are reported as having a diameter of 0.5–20 μm (Marhofer and Fritsch 2017). Furthermore, the micro-ultrasound assessed here required placement of the US transducer directly onto a resected nerve, which is clearly not feasible in clinical practice. Thus this technology will require further study and development before its clinical value becomes clear. Nevertheless, future advances in US technology are likely to improve image resolution and aid interpretation, through development of US transducers, image processing and imaging modalities (e.g. sonoelastography) (Munimara and McLeod 2013). The increasing interest in the use of artificial intelligence systems for medical image analysis is likely to extend to US used in RA. Early studies in this field are already published (Hadjerci et al. 2016), albeit much work is needed to develop these systems, and prove their accuracy and safety.

2.9 Challenges in Visualising the Needle During Ultrasound-Guided Regional Anaesthesia

Ultrasound-guided regional anaesthesia procedures largely require clear needle visualisation and fine adjustment of the needle tip. Loss of view of the needle tip, and consequent needle misplacement, can result in trauma to nerves, blood vessels (and potential intravascular injection) and damage to other nearby structures (e.g. pleura, peritoneum). Key differences in aspects of needle visibility have been demonstrated between different needles, angles of insertion and US machines (Maecken et al. 2007). For example, for every 10 degrees increase in insertion angle, for an in-plane technique, the proportion of time spent visualising the needle falls by 12% (Hebard and Hocking 2011). However this is sometimes necessitated, for example an infraclavicular brachial plexus block requires a steep angle of insertion in order to pass the needle caudad to the clavicle but posterior to the axillary artery (to reach the posterior cord of the brachial plexus). Equally, US artefact may impair visualisation. As just discussed, the posterior cord of the brachial plexus lies behind the axillary artery in the infraclavicular fossa: post-acoustic enhancement, deep to the artery, can make identification of this structure a challenging task. Also, when teaching UGRA, it is recommended to move either the needle or US probe at any one time (not both). Once the optimal view has been obtained, which visualises the needle, it is recommended that the operator does not move the US probe. However, some PNBs require movement of the probe during the procedure. For example, during the axillary level brachial plexus block, the musculocutaneous nerve is often some distance from the other nerves at the level of the block.

Finally, it is recommended that most blocks are performed ‘in plane’, i.e. the needle in line with and parallel to the US transducer probe (so

Table 2.1 Strategies to aid visualisation of the needle

Fixed probe position (rest hypothenar eminence of the probe hand on the patient)
In-plane approach
Skin insertion point close to the probe (to ease centralisation of the probe)
Avoid steep needle insertion angle (where possible)
Use of an echogenic needle
Pulse advancement of the needle
Hydrodissection
If the needle view is lost, alter the probe alignment (rather than rotation or tilt)

the tip and shaft of the needle can be visualised throughout) (Taylor and Grant 2019). However, some blocks (e.g. for catheter insertion during interscalene block) are best served using an 'out of plane' technique, i.e. needle perpendicular to the US probe (so the tip or shaft, at any point, are visualised as a hyperechoic dot). As a result, only a cross-section of the needle under the US probe is seen, with the potential that the tip of the needle may be beyond the US probe, not visualised, and causing trauma to surrounding tissues. As with nerve visualisation, ability to visualise the needle and awareness of needle tip position (especially for out-of-plane techniques) correlates positively with training and experience. Other strategies to aid needle visualisation are summarised in Table 2.1.

2.10 Technologies to Aid Visualisation

2.10.1 Needle Shaft

Larger needles are easier to visualise with US but cause greater patient discomfort – for example, a Touhy needle is often used to place a nerve catheter (Fig. 2.9). However, smaller needles provide improved patient comfort and can avoid the need altogether for applying local anaesthetic to the skin insertion site (Purushothaman et al. 2013).

A standard hypodermic needle is round in section and therefore tends to dispersion of the US waves rather than reflecting them back to the ultrasound probe. Sono-etched needles have laser grooves cut into their surface. The uneven surface allows for greater reflection of US back to the probe when compared to standard needles (van de Berg et al. 2019). This translates to a brighter signal and improved distinction from surrounding structures.

2.10.2 Needle Tip

Blunt tip needles are used in UGRA because they provide greater tactile feedback of tissue interfaces than hypodermic needles. This was particularly useful in the era of landmark and electrical stimulation techniques, prior to the widespread practice of US-guided procedures. The blunt needle causes tethering of fascial planes before advancing through them. The tissue distortion gives additional information regarding the location of the needle tip, and provides an indirect method of visualising the needle tip.

The needle tip design effects how US is reflected back to the probe, and so consequently is important in determining the needle echogenicity. Bevelled needles have been demonstrated to have greater echogenicity than conical tipped needles, and are therefore easier to visualise when using ultrasound (van de Berg et al. 2019).

There has also been interest in using bioimpedance to improve needle tip localisation and visualisation (Helen et al. 2015). The invasive measurement of tissue bioimpedance using a miniaturised electrical circuit at the tip of the needle could be used to identify the tissue type encountered.

Further recent developments of needle tip design include Onvision, a novel needle developed through collaboration between BBraun and Philips (Taylor et al. 2019). A piezoelectric crystal is incorporated into the needle 3 mm from the tip; when it lies within the US beam it interacts with the US. A signal is then generated and transmitted back to the US machine via the needle and an electrical connection. The position of the needle tip is then plotted onto the US image to aid needle tip

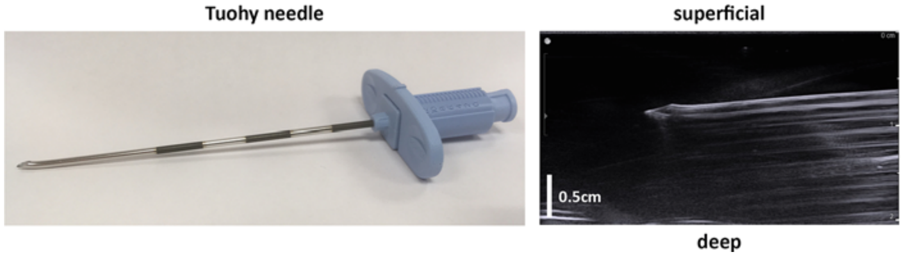

Fig. 2.9 Touhy needle
(L: photograph; R: seen on ultrasound)

localisation. This technology has been shown to improve performance of US-guided sciatic nerve blockade (Taylor et al. 2019).

2.10.3 Alignment

A key challenge of needle visualisation is alignment. For in-plane procedures the intention is to visualise all of the needle. This is only possible if the US beam is directed precisely at the needle. Several technologies have been developed to overcome this problem including probe markings, needle guides and laser guides.

Markings on the probe simply allow the operator to align the needle insertion site with the centre of the probe. The larger the probe, the more useful this becomes.

A needle guide is a device that attaches on to the US probe and facilitates one or two-dimensional movement of the needle. The needle is held in central alignment on the probe, with freedom in depth and angle of approach (on some models). This reduces the variables that confront the operator in order to perform the procedure, and has been shown in novices to reduce the time taken and improve the needle visualisation when performing a simulated US-guided nerve block (Gupta et al. 2013). However, the guide gives unwanted restriction and disruption of ergonomics for the experienced operator.

Needle alignment can be aided during US-guided PNB using a laser guide. A laser generator is attached to the US probe, with a narrow flat beam directed in the same plane as the US beam. The laser is visible on the skin to indicate the plane of the US beam. When appropriately aligned, the laser beam cannot be seen on the skin as it strikes the needle instead. Laser guides may disrupt the ergonomics by restricting how the operator can hold the US probe, but they allow for freeform movement unlike needle guides (Tsui 2007).

2.10.4 Robotic Assistance

Fully automated systems exist for venepuncture. In contrast, development of automated systems for UGRA is in its infancy. Robotic assistance provides improved probe stability and more precise needling, thus enhancing needle visualisation. However, US-guided PNBs are more time consuming using robotic assistance than freehand, although there is some evidence to suggest that robotic assistance accelerates learning (Morse et al. 2014).

2.10.5 Magnetisation

Passive needle magnetisation can be used to give a real time graphical overlay on the US image of needle tip location and needle trajectory. Magnets are embedded on the needle adding minimal bulk. This technology has been demonstrated in a porcine model to improve accuracy, especially for out of plane procedures (Johnson et al. 2017).

An external field generator can be used to create a magnetic field that induces a small current in sensors attached to the probe and needle. The current can be used to estimate needle position and direction. Again, the needle tip position and trajectory is projected onto the US image. The accuracy of this reduces with increasing distance between the field generator and the needle. However, this necessitates placing the field generator close to the patient, potentially disrupting the workflow.

2.10.6 Optical Tracking

The relative position of the needle and US transducer is determined by a camera or series of cameras, with the needle and trajectory projected on to the US image. This uses similar technology to what is used in stereotactic neurosurgery, although no clinical studies were found using this technology in regional anaesthesia. Phantom-based research has demonstrated accurate display of needle tip position and shorter procedure times. However, optical tracking is costly and direct, unobstructed camera views are required. This will restrict translation to clinical practice (Scholten et al. 2017).

2.10.7 Immersive Technology

Augmented reality is a technology that superimposes a computer-generated image on a user's view of the real world. Whilst a combination of imaging modalities may allow better for anatomical orientation, there are few examples in the literature of augmented reality applied to UGRA. One such example of applied augmented reality is in relation to epidural anaesthesia, where tracked US imaging helped to identify vertebral levels. Information was displayed on a live video feed during epidural insertion (Ashab et al. 2012). It is likely that augmented reality applications to UGRA will become most useful as educational tools.

2.10.8 Nerve Stimulation

Using nerve stimulation techniques to locate peripheral nerves was practiced widely in the UK, however this has declined with the rise of US guidance. Some clinicians still advocate its use to identify deeper nerve structures and to aid identification of inadvertent intra-neural needle tip position. Whilst the pulsed electrical stimulation may aid in the localisation of the needle tip it does not assist in visualisation. Outcomes of PNB performed under US guidance are superior to those under nerve stimulation guidance, and addition of nerve stimulation does not enhance the outcomes of UGRA (Munimara and McLeod 2015).

2.10.9 Ultrasound Technology

Movement can be used to localise the needle tip using colour Doppler imaging. This can be achieved by pulsed needle advancement (as indicated in Table 2.1), rotation of a stylet or by piezoelectric actuators. A number of needles have been designed to incorporate piezoelectric actuators that create either flexural or longitudinal vibration on application of an electrical current. With flexural vibration, the Doppler image tends to bleed into the tissue beyond the needle, resulting in difficulty in determining needle position accurately. Longitudinal mode creates only a small degree of flexural vibration. For needle design using longitudinal mode, intimate knowledge of the resonant frequency and behaviour of the block needle is required to optimally tune vibration amplitude and frequency. This minimises flexural vibration and improves needle localisation (Kuang et al. 2016).

Local anaesthetic injection creates a characteristic strain tissue strain pattern, based on the location and volume of LA injected combined with the tissue elasticity/stiffness. Elastography is an US-based technology that presents colour images of tissue strain, which can be integrated with B-mode US into a single live image. It has been demonstrated to improve the accuracy, reliability and confidence in diagnosing intraneural injection in a cohort of trainee anaesthetists, although has not yet reached widespread use in clinical practice (Munimara et al. 2016).

Tracked 2D US imaging can be reconstructed to give 3D images. This can be used to monitor the spread of LA and identify nerve catheter position, albeit not in real time. Four dimensional US refers to real time 3D imaging. In a cadaver based epidural catheter insertion study, 4D US was found to give improved operator orientation of the vertebral column, although the Touhy needle could only be reliably seen in a single imaging plane (Belavy et al. 2011). Also, compared to 2D US, 4D gives lower resolution images with lower frame rates, owing to the huge data acquisition. In turn, the operator then has the challenge of interpreting complex images.

2.11 Summary

Regional anaesthesia facilitates the delivery of anaesthesia and analgesia to an increasingly complex, elderly and co-morbid patient population. The use of ultrasound has transformed this practice, and confers significant advantages. However, it presents new challenges, including nerve and needle visualisation, and image interpretation. There are several strategies to improve image acquisition (and therefore nerve visualisation) and numerous areas of research aimed at improving needle visualisation. Image interpretation is still underpinned by sound anatomical knowledge and understanding of the typical sonographic appearance of different tissues, although advances in nerve and needle visualisation technologies aid this endeavour.

References

Ashab HA, Lessoway VA, Khallaghi S, Cheng A, Rohling A, Abolmaesumi (2012) AREA: an augmented reality system for epidural anaesthesia. Conf Proc IEEE Eng Med Biol Soc:2659–2663

Belavy C, Ruitenberg MJ, Brijball RB (2011) Feasibility study of real-time three-/four-dimensional ultrasound for epidural catheter insertion. Br J Anaesth 107(3):438–445

Bowness J, Taylor A (2019) Anatomy for the FRCA. Cambridge University Press, Cambridge. ISBN: 978-1108701884

Bowness J, Turnbull K, Taylor A, Halcrow J, Raju P, Mustafa A, Chisholm F, Varsou O, Grant C (2019) Identifying variant anatomy during ultrasound-guided regional anaesthesia: opportunities for clinical improvement. Br J Anaesth 122(5):e75–e77

Chandra A, Eisma R, Felts P, Munimara S, Corner GA, Demore CE, McLeod G (2017) The feasibility of micro-ultrasound as a tool to image peripheral nerves. Anaesthesia 72:190–196

Coventry DM, Raju PKBC (2016) Upper limb nerve blocks. Anaesth Intens Care Med 17(4):187–191

Drew T, Vo MLH, Wolfe JM (2013) The invisible gorilla strikes again: sustained inattention blindness in expert observers. Psychol Sci 24(9):1848–1853

Grant CRK (2019) Lower limb nerve blocks. Anaesth Intens Care Med 20(4):219–223

Griffin J, Nicholls B (2010) Ultrasound in regional anaesthesia. Anaesthesia 65(Suppl 1):1–12

Gupta RK, Lane J, Allen B, Sci Y, Schildcrout JS (2013) Improving needle visualization by novice residents during an in-plane ultrasound nerve block simulation using an in-plane multi angle needle guide. Pain Med 14(10):1600–1607

Hadjerci O, Hafiane A, Morette N, Novales C, Vieyres P, Delbos A (2016) Assistive system based on nerve detection and needle navigation in ultrasound images for regional anaesthesia. Expert Syst Appl 61:64–77

Hebard S, Hocking G (2011) Echogenic technology can improve needle visibility during ultrasound-guided regional anesthesia. Reg Anesth Pain Med 36(2):185–189

Helen L, O'Donnell BD, Moore E (2015) Nerve localization techniques for peripheral nerve block and possible future directions. Acta Anaesthesiol Scand 59(8):962–974

Henderson M, Dolan J (2018) Challenges, solutions and advances in ultrasound-guided regional anaesthesia. Br J Anaesth Ed 16(11):374–380

Johnson AN, Peiffer JS, Halmann N, Delaney L, Owen CA, Hersch J (2017) Ultrasound-guided needle technique accuracy: prospective comparison of passive magnetic tracking versus unassisted echogenic needle localization. Reg Anesth Pain Med 42(2):223–232

Kuang Y, Hilgers A, Sadiq M, Cochran S, Corner G, Huang Z (2016) Modelling and characterisation of an ultrasound-actuated needle for improved visibility in ultrasound-guided regional anaesthesia and tissue biopsy. Ultrasonics 69:38–46

Maecken T, Zenz M, Grau T (2007) Ultrasound characteristics of needles for regional anesthesia. Regi Anesth Pain Med 32(7):440–447

Marhofer P, Fritsch G (2017) Safe performance of peripheral regional anaesthesia: the significance of ultrasound guidance. Anaesthesia 72:427–438

Morse J, Terrasini N, Where M, Philippona C, Zaouter C, Cyr S, Hemmerling TM (2014) Comparison of success rates, learning curves, and inter-subject performance variability of robot-assisted and manual ultrasound-guided nerve block needle guidance in simulation. Br J Anaesth 112(6):1092–1097

Munimara S, McLeod G (2013) Novel applications in ultrasound technology for regional anaesthesia. Curr Anesthesiol Rep 3:230–235

Munimara S, McLeod G (2015) A systematic review and meta-analysis of ultrasound versus electrical stimulation for peripheral nerve location and blockade. Anaesthesia 70:1084–1091

Munimara S, Zealley K, Schwab A, Columba M, Corner GA, Eisma R, McLeod GA (2016) Trainee anaesthetist diagnosis of intramural injection – a study comparing B-mode ultrasound with the fusion of B-mode and elastography in the soft embalmed Thiel cadaver model. Br J Anaesth 117(6):796–800

Purushothaman L, Allan AGL, Bedforth N (2013) Ultrasound-guided ankle block. Br J Anaesth Ed 13(5):174–178

Raju PKBC, Bowness J (2019) Upper limb nerve blocks. Anaesth Intens Care Med 20(4):224–229

Smith C, Dilley A, Mitchell B, Drake R (2017) Gray's surface anatomy and ultrasound: a foundation for clinical practice, 1st edn. Elsevier, Philadelphia. ISBN 978-0702070181

Scholten HJ, Pourtaherian A, Mihajlovic N, Korsten HHM, Bouwman RA (2017) Improving needed tip identification during ultrasound-guided procedures in athletic practice. Anaesthesia 72(7): 889–904

Taylor A, Grant CRK (2019) Complications of regional anaesthesia. Anaesth Intens Care Med 20(4): 210–214

Taylor A, McKendrick M, Sadler A, Halcrow J, Raju P, Mustafa A, Seeley J, McLeod G (2019) Within-subject analysis of operator performance with and without needle tip tracking during ultrasound-guided sciatic regional nerve block on the soft embalmed Thiel cadaver. Br J Anaesth 122(3):e47–e48

Townsley P, Bedforth N, Nicholls B (2014) A pocket guide to ultrasound guided regional anaesthesia. RA-UK. ISBN 978-0992817404

Tsui BC (2007) Facilitating needle alignment in-plane to an ultrasound beam using a portable laser unit. Reg Anesth Pain Med 32(1):84–88

van de Berg NJ, Sánchez-Margallo JA, van Dijke AP, Langø T, van den Dobbelsteen JJ (2019) A methodological quantification of needle visibility and echogenicity in ultrasound images. Ultrasound Med Biol 45(4):998–1009

Varsou O (2019) The use of ultrasound in educational settings: what should we consider when implementing this technique for visualisation of anatomical structures? In Rea PM (ed) Biomedical visualisation volume 3 (1156). Series: Advances in experimental medicine and biology. Springer Nature, pp 1–11. https://doi.org/10.1007/978-3-030-19385-0_1. ISBN 978-3-030-19384-3